19ED Corium Shield

19ED.1 Issue

During a hypothetical severe accident in the ABWR, molten core debris may be present on the lower drywell (LD) floor. The EPRI ALWR Requirements Document specifies a floor area of at least 0.02 m^2/MWth to promote debris coolability. This has been interpreted in the ABWR design as a requirement for an unrestricted LD floor area of 79 m^2.

The ABWR has two drain sumps in the periphery of the LD floor which could collect core debris during a severe accident if ingression is not prevented. If ingression occurs, a debris bed will form in the sump which has the potential to be deeper than the bed on the LD floor. Debris coolability becomes more uncertain as the depth of a debris bed increases.

The two drain sumps have different design objectives. One, the floor drain sump, is designed to collect any water which falls on the LD floor. The other, the equipment drain sump, collects water leaking from valves and piping. Both sumps have pumps and instrumentation which allow the plant operators to determine water leakage rates from various sources. Plant shutdown is required when leakage rate limits are exceeded for a certain amount of time. A more complete discussion on the water collection system can be found in Subsection 5.2.5.

19ED.2 Design Description

A protective layer of refractory bricks—a corium shield—will be built around the sumps to prevent corium ingression. The shield for the equipment drain sump (EDS) will be solid except for the inlet and outlet piping which will go through its roof. The shield for the floor drain sump (FDS) will be similar except that it must have channels at floor level to allow water which falls onto the LD floor to flow into the sump. The channels will be long enough that any molten debris which reaches the inlet will freeze before it exists and spills into the sump. The width and number of the channels will be selected so that the required water flow rate during normal reactor operation is achievable. A sketch of the FDS shield is shown in Figure 19ED-1.

The walls of the EDS shield and the walls of the FDS shield without channels only have to be thick enough to withstand ablation, if any is expected to occur, for the chosen wall material. The walls of the FDS shield containing channels must be thick enough that molten debris flowing through the channels has sufficient residence time to ensure debris solidification.

Both shields extend above the LD floor to an elevation greater than the expected maximum height of the core debris bed. Thus, no significant amount of debris will collect on the shield roofs. The walls of both shields extend below the LD floor to prevent debris from tunneling under the walls and entering the sumps.

Both shields have provisions in their roofs to allow water to flow into the sumps when the lower drywell is flooded. The provisions are located next to the pedestal wall so that the debris which relocates from the vessel can not directly enter the sumps due to geometrical constraints.

Additionally, the provision for the roof of the EDS shield will not affect the normal water collection capabilities of the EDS.

To prevent the debris which falls on the lower drywell floor from directly entering the FDS shield, the channels in the FDS shield are in the walls which face away from the center of the lower drywell. The FDS shield wall which faces the center of the lower drywell is solid and does not contain any channels.

The analyses presented in Subsections 19ED.4 and 19ED.5 provide a basis for sizing the FDS shield walls with channels. The sizing of the shield walls without channels is presented in Subsection 19ED.5.3.

19ED.3 Success Criteria

The shield walls must satisfy the following requirements:

(1) Melting Point of Shield Material Above Initial Contact Temperature

The shield wall material will have a melting temperature that is greater than the interface temperature between the debris and the shield wall. Specifying alumina as the shield wall material satisfies this requirement.

(2) Channel Length

The length of the channels in the FDS shield must be long enough to ensure that a plug forms in the channel before debris spills into the sump. The freezing process is expected to take on the order of seconds or less to complete. A channel length of 0.5 meters satisfies this requirement.

(3) Shield Height Above Lower Drywell Floor

The shield height above the lower drywell floor shall be chosen to ensure long term debris solidification and to prevent debris from collecting on top of the shield. The freezing process will be complete during the time frame when the shield walls are behaving as semi-infinite solids. A height of 0.4 meters satisfies this requirement.

(4) Shield Depth Below Lower Drywell Floor

The walls of the FDS and EDS shields extend to the floors of the sumps to prevent tunneling of debris into the sumps.

(5) Channel Flow Area

The total flow area of the channels in the FDS shield shall be great enough to allow water flow rates stated in the Technical Specifications without causing excessive water pool formation in the lower drywell.

(6) Chemical Resistance of Shield Walls

The wall material chosen for the corium shields must have good chemical resistance to siliceous slags and reducing environments. Resistance can be determined to a first degree by comparing the Gibb's free energy of the oxides which make up the shield wall and the oxides present in core debris. Specifying alumina as the shield wall material satisfies this requirement.

(7) Seismic Adequacy

The seismic adequacy of the corium shields will be determined in the detailed design phase. Adequacy should be easily met because the shields are at the lowest point in the containment. Missile generation is not an issue because the shields are not near any vital equipment.

(8) Channel Height

The channel height shall be small enough to ensure freezing. The current analysis is based on a channel height of 1 cm which satisfies this requirement.

19ED.4 Channel Length Analysis

Heat transfer and phase change analyses are presented in this subsection to determine the FDS channel length which prevents molten debris ingression into the sump. A freeze front analysis is performed for early times (on the order of seconds) after vessel failure to determine the time required to form a plug. The freeze front analysis is evaluated for three debris scenarios which envelope the expected debris parameters.

19ED.4.1 Assumptions

The major assumptions invoked in the analysis and their bases follow:

(1) Molten debris enters the channel with negligible superheat.

Molten debris interacts with structural material (steel, concrete, etc.) and the lower drywell environment as it passes from the vessel, contacts the LD floor and spreads to the shield. This interaction depletes the molten debris of any superheat. To account for uncertainties, the impact of superheat will be considered in the sensitivity study contained in Subsection 19ED.4.5.2.

(2) During the freezing process, the temperature profile of the solidified debris rapidly obtains its steady state value.

This assumption introduces little inaccuracy because:

(a) The thermal conductivity of the debris is larger than that of the shield material for most debris scenarios, see Subsection 19ED.4.4.

(b) The depth of the debris is only 1 cm; thus, the thermal time constant of the debris in the channel is small compared to the freezing times. This assumption can be checked by comparing the freeze times calculated considering thermal gradients within the debris and the lumped mass analysis used in the superheat study.

(3) Heat transfer within the channel and shield is one-dimensional during plug formation.

The height of each channel is much less than its length. The heat transfer in the shield material is low enough that any heat transferred from debris contacting the shield wall outside of the channel does not affect the temperature along the channel until long after a plug has formed. Any heat transfer to the shield material between adjacent channels enhances the debris freezing process.

(4) The shield wall acts as a semi-infinite slab with an initial temperature of 330 K during the initial freezing process.

The shield material has been selected such that it is a poor conductor of heat. The penetration depth during the short duration of the freezing process is on the order of ten millimeters. The small increases in LD temperature prior to the presence of core debris does not significantly alter the shield temperature from its value during normal plant operation.

(5) Core debris is not expected to enter the LD until about two hours after accident initiation at which time the decay heat level is approximately 1% of rated power.

Core debris will not enter the lower drywell before about two hours for any credible severe accident (Subsection 19E.2.2).

(6) The decay heat generation in the debris is negligible compared to the rate of latent heat generation during the freezing process.

This assumption was verified during the analysis.

(7) The thermal conductivity and thermal diffusivity of debris in solid and liquid phases are the same.

(8) The contact resistance between the bricks was assumed to be negligible. Contact resistance will be controlled in the detailed design by varying the thickness of the bricks or by using a high temperature binder between the bricks. Thicker bricks tend

to minimize overall contact resistance by reducing the number of contact points. Some contact resistance may be acceptable in the final design if the composite thermal conductivity is high enough that the shields provide short- and long-term debris solidification.

(9) The corium shields were assumed to be structurally stable. Structural stability is only an issue during the initial onslaught of debris into the lower drywell. After debris comes into contact with the shields, a crust will form and it will tend to grow in time. Crust formation eliminates buoyancy forces and will hold the individual bricks into place.

19ED.4.2 Initial Freezing of Molten Debris in Channel

If the floor drain sump shield fulfills its design objective, a debris plug will form in the channel before a significant amount of molten corium has a chance to traverse the channel and reach the sump. Molten debris enters the channel at a significantly elevated temperature (1800 K to 2500 K) compared to the shield wall (~ 330 K). The walls absorb heat from the debris because of the large temperature difference. Since the debris contains negligible superheat, any heat loss by the debris results in freezing. Freeze fronts start at the channel walls and move toward the center of the channel. The freezing process is symmetric about the centerline of the channel because the same amount of heat is transferred through each wall while they are behaving as semi-infinite slabs. The channel walls behave as semi-infinite slabs during the freezing process because the heat conduction rate through the wall material is low compared to the release rate of latent heat. A sketch of the freezing process is shown in Figure 19ED-2.

(1) Freezing Time

The temperature profile in the crust (Reference 19ED-1), assuming it quickly reaches its steady state shape, is:

$$T_c(x) = \frac{\dot{q}L_c^2}{2k_f}\left(1 - \frac{x^2}{L_c^2}\right) + \frac{T_s - T_{f,m}}{2}\frac{x}{L_c} + \frac{T_s + T_{f,m}}{2} \qquad (19ED\text{-}1)$$

where:

$T_c(x)$ = temperature within the crust

x = vertical coordinate measured from the crust centerline

$\dot{q}$ = heat density of the debris

L_c = half thickness of the crust

k_f = thermal conductivity of debris

T_s = interface temperature between the wall and debris

$T_{f,m}$ = melting temperature of debris

The energy balance at the freeze front is:

$$q''_{lh} = -k_f \left.\frac{dT_c}{dx}\right|_{x = -L_c} \quad \text{(19ED-2)}$$

where:

q''_{lh} = the latent heat flux

The latent heat flux is:

$$q''_{lh} = \frac{dx_c}{dt}\rho_{cm} h_{lh} \quad \text{(19ED-3)}$$

where:

x_c = crust thickness

t = time

ρ_{cm} = density of debris

h_{lh} = debris latent heat of fusion

Combining these two equations, evaluating the temperature gradient and rearranging yields:

$$\frac{dx_c}{dt} = \frac{1}{\rho_{cm} h_{lh}}\left[\frac{k_f}{x_c}(T_{f,m} - T_s) - \dot{q}\frac{x_c}{2}\right] \quad \text{(19ED-4)}$$

This is a non-linear, non-homogeneous, first-order differential equation. Before effort is expended to solve it, the relative magnitudes of the terms containing the crust thickness will be determined to see if either one dominates.

The initial interface temperature between the wall of the channel and the debris can be approximated by assuming both the debris and the shield wall behave as semi-infinite solids. The resulting temperature will be somewhat less than the actual interface temperature because the freezing process will force the crust to stay closer to its initial temperature than it would if it were a semi-infinite solid body only experiencing conduction. The contact temperature between the debris and the channel wall (Reference 19ED-2), assuming semi-infinite bodies, is:

$$T_s = \frac{T_{f,m}\sqrt{(k\rho c)_{cm}} + T_i\sqrt{(k\rho c)_w}}{\sqrt{(k\rho c)_{cm}} + \sqrt{(k\rho c)_w}} \qquad (19ED\text{-}5)$$

where:

T_i = initial temperature of shield wall (assumed to be 330K)

c = specific heat

cm = debris material properties

w = wall material properties

Using the material properties for the wall and the debris contained in Tables 19ED-1 and 19ED-2, respectively, the contact temperature is estimated to be between 1475 and 2070K.

The debris energy generation density can be found by assuming a decay heat level and a total amount of corium. The density is:

$$\dot{q} = \frac{Q_{dh}\rho_{cm}}{m_{cm}} \qquad (19ED\text{-}6)$$

where:

Q_{dh} = decay heat level

m_{cm} = total mass of corium, 235 Mg.

Assuming the decay heat level is approximately 1% of rated power yields:

$$\dot{q} = 1.5 \text{ MW} / \text{m}^3$$

The two terms inside the brackets in Equation 19ED-4 can now be evaluated. For a channel height of 1 cm ($x_{c,Max}$ = 0.5 cm) and melt Scenario I (the scenario with the limiting terms) these values are:

$$\frac{k_f}{x_c}(T_{f,m} - T_s) = 9.72 \times 10^5 \text{ W/m}^2$$

$$\dot{q}\frac{x_c}{2} = 3.8 \times 10^3 \text{ W/m}^2$$

Therefore, the term containing the temperature difference across the crust is much larger than the one containing the heat generation rate. The temperature profile in the channel system ignoring energy generation in the debris is shown in Figure 19ED-2. Equation 19ED-4 can be simplified to:

$$\frac{dx_c}{dt} = \frac{k_f}{\rho_{cm} h_{lh} x_c}(T_{f,m} - T_s) \quad \text{(19ED-7)}$$

Solving this equation with the initial condition that $x_c(t = 0) = 0$, reveals:

$$x_c = \sqrt{\frac{2k_f(T_{f,m} - T_s)t}{\rho_{cm} h_{lh}}} \quad \text{(19ED-8)}$$

This equation can be rearranged to determine the time required to freeze debris in a channel of height H_o. The freezing time is:

$$t_{freeze} = \frac{H_o^2 \rho_{cm} h_{lh}}{8k_f(T_{f,m} - T_s)} \quad \text{(19ED-9)}$$

(2) Interface Temperature, T_s

The interface temperature between the debris and the channel wall can be determined by equating the heat flux from the crust to that which the crust can absorb. The heat flux from the crust is:

$$q''_{crust} = -k_f \left.\frac{dT_c}{dx}\right|_{x = x_c/2} \quad \text{(19ED-10)}$$

From Equation 19ED-1, this evaluates to:

$$q''_{crust} = \frac{\dot{q}x_c}{2} + \frac{k_f}{x_c}(T_{f,m} - T_s) \quad (19ED\text{-}11)$$

As shown previously, the temperature-difference term dominates the energy-generation term in this equation for small channel heights. Therefore, the crust heat flux can be simplified to:

$$q''_{crust} = \frac{k_f}{x_c}(T_{f,m} - T_s) \quad (19ED\text{-}12)$$

Inserting the expression for x_c in Equation 19ED-8 and rearranging yields:

$$q''_{crust} = \sqrt{\frac{k_f \rho_{cm} h_{lh}(T_{f,m} - T_s)}{2t}} \quad (19ED\text{-}13)$$

The heat flux (Reference 19ED-3) absorbed by the channel wall can be approximated by that which a semi-infinite solid body can absorb. This flux is:

$$q''_w = \frac{k_w(T_s - T_i)}{\sqrt{\pi \alpha_w t}} \quad (19ED\text{-}14)$$

where:

α_w = thermal diffusivity of the wall material

Combining Equation 19ED-13 and Equation 19ED-14 produces a relationship governing the interface temperature. It is:

$$\frac{T_s - T_i}{\sqrt{T_{f,m} - T_s}} = \left(\frac{\pi k_f \rho_{cm} h_{lh} \alpha_w}{2k_w^2}\right)^{1/2} \quad (19ED\text{-}15)$$

Solving this equation for T_s using the quadratic formula yields:

$$T_s = \frac{-(c_o - 2T_i) \pm \sqrt{(c_o - 2T_i)^2 - 4(T_i^2 - c_o T_{f,m})}}{2} \quad (19ED\text{-}16)$$

where:

c_o = the square of the right hand side of Equation 19ED-15

Negative solutions of this equation have no physical meaning. Using the material properties for the wall and the debris contained in Tables 19ED-1 and 19ED-2, respectively, the interface temperature is between 1580K and 1900K.

Since this temperature range is within the range determined for two semi-infinite bodies coming into contact, the dominance of the temperature term in Equations 19ED-4 and 19ED-11 is still valid.

19ED.4.3 Required Channel Length to Insure Freezing

The propagation rate of the freeze front was determined in form a freeze plug Subsection 19ED.4.2. This allows the determination of the time to form a freeze plug in a channel of specified height. A simple approximation of the channel length, required to provide this residence time, is the product of the initial molten debris velocity and the freezing time. This approximation would predict shield dimensions considerably larger than actually required. A more realistic channel length can be obtained by considering the reduction in channel flow area as debris freezes. In the remainder of this subsection, the following parameters will be determined:

- debris velocity at channel entrance,
- channel area decrease resulting from debris freezing,
- average channel debris velocity, and
- the required channel length to insure plug formation at the channel entrance before corium ingression into the sump.

(1) Debris Velocity at Channel Entrance

The possibility exists that molten debris will not even enter the channel after it has come into contact with the shield wall. Debris which is spreading across the lower drywell floor will have at least a thin crust formed on its leading edge. If the flow energy of the advancing debris front is not great enough to break this crust and overcome surface tension on the length scale of the channel height, debris will not enter the channel. Unfortunately, the physics of crust formation is not currently understood well enough to support this argument without a great deal of uncertainty.

Since the channels are in shield walls which are not facing the center of the lower drywell, the entrance velocity is governed by the height of corium outside of the channel. Assuming that the debris spreads uniformly across the lower drywell floor, the height of debris can be obtained by integrating the volumetric expulsion rate of corium from the vessel divided by the floor area of the lower drywell. The expulsion rates for three scenarios will be considered in Subsection 19ED.4.4. The three scenarios cover the spectrum of core melt phenomena and debris properties.

The velocity at the channel entrance can be conservatively over predicted by ignoring frictional effects. Frictional effects should actually be quite large because the viscosity of the debris will increase dramatically as it freezes. This velocity is:

$$v_e(t) = \sqrt{2g\Delta z(t)} \qquad \text{(19ED-17)}$$

where:

v_e = velocity at the entrance of the channel

g = gravitational acceleration constant

Δz = height of debris in the lower drywell

Expanding debris height yields:

$$v_e(t) = \sqrt{\frac{2g\dot{m}_{ves}}{\rho_{cm} A_{ld}}\, t} \qquad \text{(19ED-18)}$$

where:

$\dot{m}_{ves}$ = ejection rate of corium from a failed vessel

A_{ld} = floor area of the lower drywell, 79 m^2 minimum

(2) Channel Area Decrease Resulting From Debris Freezing

The mass flow rate of corium in the channel decreases in time due to the area reduction resulting from debris freezing. A conceptual picture of this area reduction process is shown in Figure 19ED-3. The mass flow rate at the entrance of the channel and at the location downstream where the debris front has just arrived is:

$$\dot{m}_i(t) = \rho_{cm} v_e(t) H_i(t) = \rho_{cm} v_o(t) H_o + \dot{m}_{fr} \qquad \text{(19ED-19)}$$

where:

$\dot{m}_i$ = time varying mass flow rate per unit width at the entrance of the channel

H_i = time varying entrance flow height of the channel

v_o = time varying velocity at the downstream location in the channel where molten debris has just arrived

H_o = unobstructed height of the channel

$\dot{m}_{fr}$ = mass freezing rate of debris per unit width in the channel

This equation requires that:

$$v_o(t) = \frac{v_e(t)}{H_o} H_i(t) - \frac{\dot{m}_{fr}}{\rho_{cm} H_o} \tag{19ED-20}$$

The entrance flow height is:

$$H_i(t) = H_o - 2x_c(t) \tag{19ED-21}$$

Inserting the relationship for x_c found in Equation 19ED-8 into this expression yields:

$$H_i(t) = H_o - \sqrt{\frac{8k_f(T_{f,m} - T_s)t}{\rho_{cm} h_{lh}}} \tag{19ED-22}$$

The product of this equation and the width of the shield channel describes the reduction of channel inlet flow area with time.

(3) Average Channel Debris Velocity

The velocity of the leading edge of molten debris in the channel can be obtained by combining Equations 19ED-18, 19ED-20 and 19ED-22. It is:

$$v_o(t) = a_o\sqrt{t} - \frac{2a_o b_o}{H_o} t - \frac{\dot{m}_{fr}}{\rho_{cm} H_o} \tag{19ED-23}$$

where:

a_o = $\sqrt{\frac{2g\dot{m}_{ves}}{\rho_{cm} A_{ld}}}$

$$b_o = \sqrt{\frac{2k_f(T_{f,m} - T_s)}{\rho_{cm} h_{lh}}} \quad \text{(19ED-24)}$$

The average velocity of debris between the entrance of the channel and the leading edge of molten corium is:

$$\bar{v}(t) = \frac{\int_0^t v_o(t)dt}{\int_0^t dt} \quad \text{(19ED-25)}$$

Evaluating this integral yields:

$$\bar{v}(t) = \frac{2}{3}a_o\sqrt{t} - \frac{a_o b_o}{H_o}t - \frac{1}{t}\int_0^t \frac{\dot{m}_{fr}}{\rho_{cm} H_o}dt \quad \text{(19ED-26)}$$

This is the time averaged velocity of the molten debris in the shield channel.

(4) Mass of Debris Frozen in Channel

The time varying mass of debris freezing in the channel per unit width can be approximated by

$$\dot{m}_{fr} = \frac{d}{dt}(A'\rho_{cm}) \quad \text{(19ED-27)}$$

where:

A' = cross sectional area of frozen debris

The cross sectional area can be related to the crust thickness by modifying Equation 19ED-8 to account for the variable residency time of the debris at various vertical locations in the channel. This process yields

$$A' = 2b_o\int_o^L \sqrt{t - \frac{y}{\bar{v}(t)}}dy \quad \text{(19ED-28)}$$

where:

L = length from the channel entrance to the leading edge of the debris front

y = vertical coordinate measured from the entrance of the channel

Evaluating this integral yields:

$$A' = \frac{4}{3} b_o \bar{v}(t) t^{3/2} \tag{19ED-29}$$

Combining this result with Equations 19ED-25 and 19ED-26 yields:

$$\bar{v}(t) = \frac{2}{3} a_o \sqrt{t} - \frac{a_o b_o}{H_o} - \frac{4 b_o \bar{v}(t)}{3 H_o} \sqrt{t}$$

$$= \frac{\frac{2}{3} a_o \sqrt{t} - \frac{a_o b_o}{H_o} t}{1 + \frac{4 b_o}{3 H_o} \sqrt{t}} \tag{19ED-30}$$

(5) Required Channel Length to Insure Freezing

The channel length, required to ensure a plug forms at the channel entrance before debris spills into the sumps, is:

$$L_{freeze} = \bar{v}(t_{freeze}) t_{freeze} \tag{19ED-31}$$

where t_{freeze} is given by Equation 19ED-9.

19ED.4.4 Channel Lengths for Different Melt Scenarios

The analysis to determine the channel length required to ensure that a plug forms in the channel prior to debris entering the sump is contained in Subsection 19ED.4.3. The analysis will be executed in this subsection for three different melt scenarios which cover the range of expected core melt conditions. The scenarios differ in debris composition, debris material properties, initial temperature of the debris and the ejection rate of debris from the failed vessel. The impact of debris superheat will be considered in a sensitivity study contained in Subsection 19ED.4.5.2.

Scenarios I and II were taken from NUREG/CR-5423 (Reference 19ED-7). These scenarios represent predominantly oxidic and metallic melts, respectively. The Peach Bottom Atomic Power Station was used for specifics in the NUREG/CR-5423 calculations. However, the similarities between Peach Bottom and the ABWR in core composition and vessel geometry allow the NUREG/CR-5423 core melt parameters to be applied in this analysis.

Scenario I is based on MAAP calculations which predict that there is a significant amount of molten debris available for relocation at the time of vessel failure. The debris release in this scenario is consistent with the core composition, corresponding to approximately 30% by weight of zirconium. Further, 20% of the available zirconium was assumed to be oxidized.

Scenario II is based on BWRSAR calculations which predict that debris which initially relocates to the lower plenum of the vessel is quenched. Subsequent water depletion results in the remelting of the debris and local failure of the vessel. Since the metallic constituents of the debris remelt before the oxidic constituents, the initial debris pour from the vessel is primarily metallic.

For both scenarios, only the initial molten material relocation is important in determining the required channel length because the channels will plug in a relatively short period of time (less than 10 seconds). Only the maximum initial debris relocation rates were utilized so that the calculated channel lengths would be conservatively over-estimated. Subsequent molten material releases from the vessel will go into filling the lower drywell with debris and have no bearing on plug formation. Thus, the long-term debris relocation parameters discussed in NUREG/CR-5423 are of no consequence to this analysis.

The third scenario considered, Scenario M, represents the MAAP-ABWR analysis that was used to predict a bounding debris ejection rate from a failed oxidic vessel, see Subsection 19EB.6.2.2. MAAP-ABWR predicts that the mass flow rate from the vessel jumps to approximately 1000 kg/s at vessel failure and then increases to 6000 kg/s in eight seconds, see Figure 19EB-9. The debris release is essentially complete (flow rate 0 kg/s) in ten seconds. In order to avoid determining the debris entrance velocity into the channel for this complicated flow rate profile, the maximum debris relocation rate was assumed to prevail throughout the plug formation process. This assumption will lead to a conservative over-estimation of the required channel length.

Another melt scenario commonly considered in calculations involving ex-vessel core debris is the formation of eutectics as a result of core-concrete interactions. However, consideration of eutectics is not required in the analysis of plug formation. In order for the debris properties to be changed significantly, core-concrete interactions must increase the debris mass by at least 10%. The time required for this to happen is longer than the time required for plug formation for a quickly spreading debris front. Alternatively, if the debris front is spreading slowly enough to allow a significant amount of core-concrete interaction, the leading edge of the debris will have a thick crust and have a height greater than the channel height. Thus, debris will not even enter the channel.

The parameters describing each of the three scenarios considered is contained in Table 19ED-2. The debris material properties for Scenarios I and II were determined using the constituent material properties contained in Table 19ED-3. Material properties for Scenario M were taken from MAAP-ABWR.

Inserting the scenario parameters contained in Table 19ED-2 into the analysis contained in Subsection 19ED.4.3 results in the channel lengths contained in Table 19ED-4. All of the required channel lengths are less than 0.5 meters.

19ED.4.5 Sensitivity to Melt Parameters

The three scenarios considered in Subsection 19ED.4.4 were chosen to represent a wide range of possible debris characteristics. The calculation of required channel length depends on the debris flow rate, the debris temperature, the channel height and several material properties of the debris and wall material. This subsection will evaluate the sensitivity of the calculation to these parameters. The final part of this subsection will evaluate the impact of debris superheat.

19ED.4.5.1 Material Properties

The channel length required to ensure freezing is dependent on both debris and channel wall material properties. The relevant debris material properties are density, latent heat of fusion and thermal conductivity. For the channel wall, the relevant properties are thermal conductivity and thermal diffusivity. The sensitivity of the channel length calculation to these material properties will be determined in this subsection. Additionally, the sensitivity to debris temperature and debris flow rate from the vessel will also be determined.

The sensitivity of the channel length calculation to these parameters will be estimated by varying each parameter, except debris temperature, by ± 20%. Debris temperature will be varied by ± 200K. The wide variations in material properties of the three base scenarios take into account deviations outside of this range and combinations of deviations.

The results of varying these parameters are contained in Table 19ED-5. The following discussion will describe the effect on channel length due to increasing each parameter. The reverse of the effect described holds true for decreasing the parameter.

Increasing debris density, latent heat of fusion or flow rate increases the amount of energy that must be transferred to the channel walls before a plug forms, and, as a result, increases the required channel length. Increasing the debris thermal conductivity increases the rate at which the debris can transfer its energy, and decreases the required channel length. Increasing the debris temperature increases the debris to channel wall temperature difference and, as a result, the rate of heat loss by the debris. Since this analysis assumes that the debris enters the channel with negligible superheat, increasing the debris temperature reduces the required channel length.

The impact on channel length due to variations in wall material properties is a direct result of the change in the interface temperature between the debris and the channel wall. Increasing the wall thermal conductivity decreases the interface temperature and results in a shorter channel length. Conversely, increasing the wall thermal diffusivity increases the interface temperature and results in a longer channel length.

Decreasing the interface temperature increases the temperature difference driving heat flow from the debris, and results in more rapid freezing. Alternatively, increasing the interface temperature decreases the interface temperature, and results in a longer freezing length. The interface temperature is decreased by increasing wall conductivity and increased by increasing wall thermal diffusivity. Thus, increasing the wall thermal conductivity decreases the required channel length, while the opposite is true for increasing wall thermal diffusivity.

The three parameters which have the largest impact on channel length are debris density, debris latent heat of fusion and wall thermal conductivity. The impact of the debris properties are not surprising because they directly impact the amount of energy that must be removed from the debris in order for plug formation to occur. The impact of decreasing the thermal conductivity of alumina does not need to be considered because a lower bound of alumina thermal conductivity was used in the base analysis. Thus, a ten-percent decrease in the wall thermal conductivity is physically unrealistic.

As can be seen in Table 19ED-5, none of the parameter variations for Scenarios I and II resulted in required channel lengths greater than 0.5 meters. Only two of the variations for Scenario M resulted channel lengths greater than 0.5 meters, and these channel lengths were only slightly greater. If the channels are 0.5 meters long and two meters wide, the amount of debris which could enter the sump for a Scenario M melt with these two parameter variations is approximately 0.001 m^3 (average depth 0.03 cm). This amount of debris entering the sump does not pose a threat to containment integrity Therefore, a channel length of 0.5 meters supplies enough margin to account for uncertainties in material properties.

19ED.4.5.2 Impact of Superheat

The channel length analysis contained in Subsection 19ED.4.3 assumes that the debris enters the channel with negligible superheat. The analysis contained in this subsection considers the effects of superheat on the corium freezing process. First, the credible amount of superheat for each melt scenario is discussed. Then, the change in energy due to including superheat will be calculated. Next, the impact on freezing time will be determined. The analysis will conclude with the determination of channel length when superheat is present.

According to NUREG/CR-5423 (Reference 19ED-7), the initial superheat of Scenario I is expected to be negligible “because of several concurrent reasons: (a) convective heat transfer to boundaries--typically less than 100 °C can be sustained at decay heat levels, (b) continuous melting and incorporation of boundary material, and (c) heat losses to water and control rod guides during the relocation through the lower plenum.” The upper bound of reasonable

superheat that the debris could obtain at the time of vessel failure was specified to be 125 °C. The most probable superheat was limited to less than 50 °C. Due to similarities in Scenario I and Scenario M (quick penetration failure after delayed core plate failure and mostly oxidic melt), the superheat of the two cases can be assumed to be the same.

Scenario II is expected in NUREG/CR-5423 to have more superheat than Scenario I because the molten mass does not have as much opportunity to lose heat to the lower head. The upper bound of reasonable superheat that the Scenario II debris could obtain at the time of vessel failure was specified to be 150 °C. The most probable superheat was limited to less than 100 °C.

After the debris exits the vessel in any of the scenarios, the debris will lose some of its heat before it reaches the corium shields. The heat loss will be by radiation and convection to the lower drywell environment and structures. Additionally the debris pool on the lower drywell floor will conduct heat to the lower drywell floor. These heat losses will remove some, if not all, of the debris superheat. This analysis conservatively assumes that the debris enters the shield wall channels with the same superheat it had when exiting the vessel.

19ED.4.5.2.1 Change in Energy

The fractional change in debris energy due to adding superheat can be obtained by comparing the energy content of the debris with superheat to the energy content without superheat. This yields

$$E_{change} = \frac{mh_{lh} + mc_p\Delta T}{mh_{lh}} = \frac{c_p\Delta T}{h_{lh}} \quad \text{(19ED-32)}$$

where:

m = mass of debris to be frozen

c_p = heat capacity of debris

ΔT = amount of superheat

Table 19ED-6 shows the percent change in energy which results from assuming different amounts of superheat for the three scenarios. The energy comparison indicates that a significant amount of superheat (greater than 25 °C) could impact the channel length. However, for superheats on the order of a few degrees, there is negligible impact.

19ED.4.5.2.2 Channel Length with Superheat

A simplified analysis of the channel length required to ensure plug formation before debris ingression into the sumps will be presented in this subsection. The superheat temperature will be assumed to decrease the fusion point of the melt, not increasing the temperature of the melt exiting the vessel. This will conservatively result in longer required channel lengths, as indicated by Subsection 19ED.4.5.1.

The alternative manner of accounting for superheat is increasing the temperature of the debris. This results in a shorter channel length because the interface temperature increases compared to the case in which the fusion point is decreased. The interface temperature for all three scenarios resulting from adding the upper bounds of superheat are less than 1975K. This temperature is less than the melting temperature of alumina. Therefore, adding superheat to the debris temperature results in a shorter freezing length without thermally degrading the channel walls. The remainder of this analysis will conservatively account for superheat by decreasing the solidus temperature.

Balancing the energy required to be removed from the debris to freeze and the energy to be absorbed by the shield wall, assuming that the debris in the channel behaves as a lumped mass, yields

$$t_{freeze} = \frac{e''_f}{\bar{q}''_w}$$

where e''_f = energy required to be removed from the debris in order for freezing to occur

$$= \frac{H_o \rho_{cm}}{2}(h_{lh} + c_p \Delta T) \qquad \text{(19ED-33)}$$

$\bar{q}''_w$ = time averaged heat flux into either the upper or lower channel wall (semi-infinite body), see Equation 19ED-14 for the instantaneous heat flux

$$= \frac{2k_w(T_s - T_i)}{\sqrt{\pi \alpha_w t}} \qquad \text{(19ED-34)}$$

Combining all the portions of this equation yields

$$t_{freeze} = \left[\frac{H_o \rho_{cm}(h_{lh} + c_p \Delta T)\sqrt{\pi \alpha_w}}{4k_w(T_s - T_i)}\right]^2 \quad \text{(19ED-35)}$$

The plug formation time for the three scenarios is presented in Table 19ED-7 for various amounts of superheat. Note that this equation produces the same result as Equation 19ED-9 if there is no superheat.

The average velocity in the channel can be obtained by following the same methodology used in Subsection 19ED.4.3 for the case without superheat. Performing this analysis yields

$$\bar{v} = \frac{\frac{2}{3}a_o\sqrt{t} - \frac{a_o b'_o}{H_o}t}{1 + \frac{4b'_o}{3H_o}\sqrt{t}}$$

$$\text{where} \quad b'_o = \frac{2k_w(T_s - T_i)}{\rho_{cm}(h_{lh} + c_p \Delta T)\sqrt{\pi \alpha_w}} \quad \text{(19ED-36)}$$

Note that this equation and Equation 19ED-29 are identical except for the definition of the parameter b_o which describes the ratio of heat removal capability to the energy that must be removed for freezing to occur. The channel length required to ensure freezing is simply the product of the average velocity and the freezing time.

The required channel lengths for each of the three scenarios is shown in Table 19ED-8 for various amounts of superheat. All of the Scenario I and II required channel lengths are less than 0.5 meters. The required channel lengths for Scenario M exceed 0.5 meters for superheats greater than approximately 70 °C. However, for a channel length of 0.5 meters, the amount of debris that can enter the sump under these conditions is small. The average velocity of the debris in the channel for the Scenario M is less than approximately 0.1 m/s. Assuming that the total channel width is 2 meters, the amount of debris that can enter the sump is less than 0.006 m^3(0.2 cm average depth) for superheats up to 125 °C. This amount of debris entering the sump does not pose a threat to containment integrity.

19ED.4.5.2.3 Conclusion of Superheat Impact

A channel length of 0.5 meters will prevent significant debris ingression into the sumps for credible superheats in all three debris scenarios. No debris is expected to enter the sump for either the Scenario I or II melts, while a small amount may enter for Scenario M melts for superheats in excess of 70 °C. Based on the methodology of NUREG/CR-5423, the superheat

in Scenario M type melt is probably limited to less than 50 °C. For Scenario M melts with superheats outside the probable range, only a small amount of debris will enter the sump and the average depth will be limited to approximately 0.2 cm. Therefore, the corium shield for the floor drain sump will perform its function even if the core debris exiting the vessel is superheated.

19ED.4.6 Conclusion of Channel Length Analysis

A channel length of 0.5 meters provides adequate assurance that molten debris that enters the floor drain sump corium shield will form a plug prior to debris spilling into the sump. Three debris melt scenarios were considered which bound the credible melt compositions and the credible debris ejection rates from the vessel. Two of the scenarios represented the oxidic and metallic melts used in the Mark I liner failure analysis, NUREG/CR-5423. The third scenario was developed with MAAP-ABWR to provide a gross over-estimation of the maximum debris ejection rate from a failed vessel. A sensitivity analysis demonstrated that a channel length of 0.5 meters provides enough margin to account for uncertainties in material properties. Additionally, the impact of superheat was shown to be minimal.

19ED.5 Long-Term Capability of the Shield Walls

Initial debris solidification was considered in Subsection 19ED.4. The requirements for keeping the debris in the channel frozen for an extended period of time (at least 24 hours) will be determined in this subsection. The height of the upper shield walls (above the lower drywell floor) with channels and depth of the lower shield walls (below the lower drywell floor) with channels will be specified. Additionally, the thickness of the shield walls without channels will be specified.

19ED.5.1 Upper Shield Wall (Above Lower Drywell Floor) with Channels

To help assure the integrity of the roof of the corium shield, the upper shield wall should be tall enough to prevent the debris that is collecting on the lower drywell floor from flowing on top of the shield. Debris falling directly on the roof during relocation from the vessel does not pose a threat to roof integrity because the amount of debris that can fall on the roof is small. This is a result of the CRD and lower drywell configurations. The length and density of the CRDs in the lower drywell prevents the debris from exiting the CRD grid with any significant horizontal velocity component. The sumps are on the periphery of the lower drywell floor. Thus, debris which relocates from the vessel will not fall directly on the sump roofs.

To prevent any debris from flowing on top of the shield roof, the shield should be taller than the maximum possible debris pool depth in the lower drywell. This requirement is given by:

$$H_{uw} \geq \frac{m_{cm,\,tot}}{\rho_{cm} A_{ld,\,min}} \qquad \text{(19ED-37)}$$

where:

$m_{cm,tot}$ = maximum amount of corium, 235 Mg

$A_{ld,min}$ = minimum floor area of the lower drywell, 79 m^2

Evaluating this expression yields:

$$H_{uw} \geq 0.33 \text{ m} \qquad \text{(19ED-38)}$$

After debris relocation into the lower drywell, the lower drywell will almost always be flooded with water either by active systems (e.g., the firewater addition system) or by the passive flooder. The probability that the lower drywell will not be flooded after debris relocation is extremely small and is low enough that the case of a non-flooded lower drywell can be excluded from consideration.

The water in the lower drywell will provide long-term cooling to the debris on the floor, to any debris that is on the roof of the corium shield, and to the corium shield walls. Additionally, since the roof of the corium shield allows water flow into the sump when the lower drywell is flooded, the inner walls of the shield will be cooled. The heat transfer from the shield walls to the water is effective in preventing the debris frozen in the channels from remelting. Therefore, if the lower drywell is flooded, long-term solidification of the debris in the channels is assured and debris ingression into the sump is prevented.

To meet the requirements set forth in this subsection, the upper shield wall is specified to be 0.4 meters.

19ED.5.2 Lower Shield Wall (Below Lower Drywell Floor) with Channels

As stated in Subsection 19ED.5.1, long-term solidification of the debris in the channels is assured due to heat transfer from the shield walls to the water which has filled the lower drywell due to initiation of an active system or the passive flooder. Therefore, the only requirements for the lower shield wall are to absorb the initial energy released by the debris during the freezing process and to prevent tunneling of the debris beneath the shield when significant core-concrete interaction has not already occurred.

During the freezing process, the channel walls behave as semi-infinite bodies with a temperature penetration depth less than a centimeter. Thus, the lower shield wall needs to have a depth of at least one centimeter to meet the requirement for initial debris freezing.

If core-concrete interaction is occurring, the potential exists that the lower drywell floor will be eroded to a depth below the lower shield wall. If this occurs, the debris could tunnel into the sump. This concern is eliminated by specifying that the shield wall extends down to the floor of the sump.

19ED.5.3 Shield Walls without Channels

The discussion in most of this attachment has focused on the shield walls with channels. This subsection will address the requirements for the shield walls without channels. The thickness, height and depth will be specified.

The corium shield walls without channels only need to be thick enough to provide a long-term, stable interface between the debris on the lower drywell floor and the interior of the sumps. As discussed in Subsection 19ED.5.1, only the long-term scenario with a flooded lower drywell needs to be considered.

The wall thickness needed to transfer a given heat flux under steady-state conditions is

$$\Delta w = \frac{kw(T_{w,o} - T_{w,i})}{q''_d} \qquad \text{(19ED-39)}$$

where:

$T_{w,o}$ = surface temperature of wall in contact with debris

$T_{w,i}$ = surface temperature of wall on inside of shield, and

q''_d = heat flux from the debris.

Assuming that the water in the sump is at three atmospheres, the inner shield wall will achieve a temperature of approximately 410 K to allow nucleate boiling. The MAAP-ABWR analysis contained in Subsection 19E2.2 demonstrate that the typical drywell pressure at the time of vessel failure is three atmospheres. To avoid ablation, the wall surface temperature in contact with debris must be less than the melting temperature of the shield wall material (approximately 2280 K for alumina).

The heat flux from the debris bed in the lower drywell can be approximated by assuming that the decay heat level is one-percent and that all the surfaces of the bed have the same heat flux. This approximation yields:

$$q''_d = 250\ \text{kW/m}^2. \qquad \text{(19ED-40)}$$

The actual heat flux to the wall may be significantly lower due to enhanced heat transfer from the debris bed to the overlying pool of water or separation of the bed from the wall.

Evaluating the wall thickness for these conditions yields

$$\Delta x = 3\ \text{cm}. \qquad \text{(19ED-41)}$$

This wall thickness provides a stable interface between the debris bed and a water filled sump. If the wall is thicker, it will ablate to this thickness and then establish a stable interface. To provide margin for any erosion due to initial debris contact with the wall, the thickness of the shield walls without channels is specified to be 10 cm.

The reasoning contained in Subsections 19ED.5.1 and 19ED.5.2 regarding the height and depth of the shield walls with channels also applies to the walls without channels. The height of the shield walls should be 0.4 meters which is greater than the maximum height of the debris bed in the lower drywell. The shield walls should extend to the floor of the sump to prevent debris tunneling.

19ED.6 Related Experimental and Analytical Work

The freezing of molten fuel in narrow channels and tubes has been studied previously in regards to core disruptive accidents in liquid metal fast breeder reactors (References 19ED-10, 19ED-11, 19ED-12 and 19ED-13) and in regards to ceramic core retention devices (Reference 19ED-13). This subsection will review these works for application to the channel freezing analysis contained in Subsection 19ED.4.

Cheung and Baker (Reference 19ED-10) analytically and experimentally studied the transient flow and freezing of molten core debris in coolant channels of a liquid-metal fast breeder reactor. Their data analysis determined the impact of several parameters on the penetration depth of the fuel into the channel. The derived variations are in general agreement with the trends shown in the sensitivity study contained in Subsection 19ED.4.5. This work culminated in the determination of penetration depths for several coolant channel diameters. The material properties of Scenario M compare somewhat favorably to the material properties used by Cheung and Baker. However, they used a channel flow velocity of 100 cm/s. Modifying their results to account for velocity differences yields penetration distances from 20 to 66 cm for channel diameters between 0.64 and 1.27 cm and a debris temperature of 2770 °C. This result compares well to the results determined for Scenario M—a penetration depth of 30 cm for a 1 cm channel.

Fieg, et. al., (Reference 19ED-12) performed channel plugging experiments at the Karlsruhe THEFIS facility in Germany using alumina and alumina-iron melts as fuel simulants. The results indicated that the conduction-limited crust growth is an adequate hypothesis for modeling the penetration and freezing of molten fuel. The basis of the this crust-growth model is that a stable crust forms at the channel boundary and then grows continually until it clogs the channel. This is also the basis of the model developed in Subsection 19ED.4. The experimental results presented by Fieg cannot readily be compared to the corium shield because the experimental velocities are so much higher (2.2 m/s to 4.4 m/s compared to 0.01 m/s to 0.1 m/s). However, Fieg's findings that increasing wall temperatures and/or driving pressures increases penetration depth are consistent with the model developed in Subsection 19ED.4.

Soussan, et. al., (Reference 19ED-11) compared the results of experiments performed at AAE Winfrith and CEN Grenoble with the BUCOGEL code developed at Cadarache. The comparison revealed that penetration depths are over predicted using the conduction freezing model and under predicted using the bulk freezing model. The freezing of UO_2 was shown to be consistent with the conduction freezing mode. Alternatively, freezing of molybdenum was determined to undergo bulk freezing. This would tend to indicate that the analysis in Subsection 19ED.4 over predicts the freezing of metallic melts such as Scenario II. However, the overall impact to the analysis is negligible because Scenario II is not limiting.

PLUGM (Reference 19ED-13) was developed to analyze freezing in a variety of geometries including the gaps between the ceramic bricks of a core retention device. The model in 19ED.4 is similar to the PLUGM model for "Thin Slit Geometry - No Crust with a Nonmelting, Infinitely-Thick Wall". The primary difference is that 19ED.4 is somewhat more simplified to allow a closed-form analytical solution, whereas PLUGM must be solved numerically. Unfortunately, the example contained in Reference 19ED-13 for a thin slit geometry does not lend itself to comparison with the corium shield analysis because the example models a vertical channel with a high entrance velocity.

The past investigations into the freezing of molten fuel in narrow channels tend to support the modeling and results of the channel length analysis contained in Subsection 19ED.4.

19ED.7 References

19ED-1 Frank P. Incropera and David P. DeWitt, "Fundamentals of Heat and Mass Transfer", 2nd Ed., John Wiley and Sons, 1985, pp. 85-86.

19ED-2 Glen E. Myers, "Analytical Methods in Conduction Heat Transfer", Genium Publishing Corp., Schenectady, NY, 1987, p. 202.

19ED-3 Frank P. Incropera and David P. DeWitt, "Fundamentals of Heat and Mass Transfer", 2nd Ed., John Wiley and Sons, 1985, p. 203.

19ED-4 Frank P. Incropera and David P. DeWitt, "Fundamentals of Heat and Mass Transfer", 2nd Ed., John Wiley and Sons, 1985, pp. 433-435.

19ED-5 H.S. Carslaw and J.C. Jeager, "Conduction of Heat in Solids", 2nd Ed., Oxford University Press, 1959, pp. 112-113.

19ED-6 "Mark's Standard Handbook for Mechanical Engineers", 8th Ed., Theodore Baumeister, Editor-in-Chief, McGraw-Hill Book Company, 1978, pp. 6-171 to 6-177.

19ED-7 T.G. Theofanous, W.H. Amarasooriya, H. Yan, and U. Ratnam, "The Probability of Liner Failure in a Mark-I Containment", NUREG/CR-5423, August 1991.

19ED-8 "MAAP-3.0B Computer Code Manual", EPRI NP-7071-CCML, November 1990.

19ED-9 "CRC Handbook of Chemistry and Physics", 62nd Ed. CRC Press, Boca Raton, Florida, 1981.

19ED-10 F.B. Chueng and L. Baker, "Transient Freezing of Liquids in Tube Flow, Nuclear Science and Engineering", 60, pp. 1-9, 1976.

19ED-11 P. Soussan, M. Schwartz, D. Maxon, and B. Berthet, "Propagation and Freezing of Molten Material Interpretation of Experimental Results", Proceedings of the 1990 International Fast Reactor Safety Meeting, Snowbird, Utah, August 12-16, 1990.

19ED-12 G. Fieg, M. Möschke, I. Schub and H. Werle, "Penetration and Freezing Phenomena of Ceramic Melts Into Pin-Bundles", Proceeding of the 1990 International Fast Reactor Safety Meeting, Snowbird, Utah, August 12-16, 1990.

19ED-13 M. Pilch and P.K. Mast, "PLUGM: A Coupled Thermal-hydraulic Computer Model for Freezing Melt Flow in a Channel", NUREG/CR-3190, SAND82-1580, Sandia National Laboratories, Albuquerque, NM 1982.

Table 19ED-1 Material Properties

Property	Alumina (Reference 19ED-6)	Concrete
Melting Temperature (K)	2280	1450
Density (kg/m^3)	2700	2300
Thermal Conductivity (W/m•K)	4-8	1.3
Specific Heat (J/kg•K)	1000	800
Thermal Diffusivity (m^2/s)	1.48×10^{-6}	7.5×10^{-7}

Table 19ED-2 Scenario Parameters

	Scenario I*	Scenario II	Scenario M†
Flow Rate (m^3/min)	4	0.7	42
Debris Temperature (K)	2850	1800	2500
Composition (w/o):			
UO_2	70	4	61
ZrO_2	10	0	3
Zr	20	47	24
Fe	0	35	~
Cr	0	8	~
Ni	0	6	~
Carbon steel‡	~	~	12
Material Properties:			
Density (kg/m^3)	8900	7300	8500
Specific heat (J/kgK)	960	705	800
Thermal conductivity (W/mK)	6	26	12
Heat of fusion (MJ/kg)	0.31	0.26	0.28

* Scenarios I and II correspond to the Scenarios I and II defined in NUREG/CR-5423 (Reference 19ED-7).

† Scenario M corresponds to the MAAP-ABWR case run to bound debris ejection rate, see Subsection 19EB.6.2.2.

‡ MAAP uses carbon steel instead of its constituents Fe, Cr and Ni.

Table 19ED-3 Constituent Material Properties*

	Density (kg/m^3)	Specific Heat (J/kgK)	Thermal Conductivity (W/mK)	Heat of Fusion (MJ/kg)
UO_2	10100	1000	3.3	0.27
ZrO_2	5600	991	3	0.71
Zr	6500	780	18	0.25
Fe	7800	570	35	0.27
Cr	7200	781	35	0.26
Ni	8900	609	35	0.30
carbon steel†	8000	795	35	0.25

* Material properties from NUREG/CR-5423 (Reference 19ED-7), MAAP User's Manual (Reference 19ED-8) and the CRC Handbook (Reference 19ED-9)

† MAAP uses carbon steel instead of its constituents Fe, Cr and Ni.

Table 19ED-4 Results of Channel Length Calculation

	Scenario I	Scenario II	Scenario M
Interface Temperature (K)	1880	1580	1900
Freeze Time (s)	5.7	4.2	4.2
Channel Velocity (m/s)	0.03	0.01	0.07
Required Channel Length (m)	0.18	0.05	0.35

Table 19ED-5 Effect of Parameter Variations

	Channel Length (m)			
	Scn I	Scn II	Scn M	Average Effect
Base Case	0.18	0.05	0.35	
Debris:				
Density + 20%	0.26	0.07	0.50	+33%
Density – 20%	0.11	0.03	0.24	–63%
Latent heat of fusion + 20%	0.26	0.07	0.55	+35%
Latent heat of fusion – 20%	0.11	0.03	0.21	–69%
Flow rate + 20%	0.19	0.05	0.39	+9%
Flow rate – 20%	0.16	0.04	0.32	–12%
Thermal conductivity + 20%	0.15	0.04	0.32	–12%
Thermal conductivity – 20%	0.21	0.05	0.41	+13%
Temperature + 200K	0.15	0.03	0.29	–27%
Temperature – 200K	0.21	0.07	0.45	+23%
Wall:				
Thermal conductivity + 20%	0.14	0.03	0.26	–36%
Thermal conductivity – 20%	0.25	0.08	0.53	+34%
Thermal diffusivity + 20%	0.20	0.06	0.42	+15%
Thermal diffusivity – 20%	0.15	0.04	0.30	–21%

Table 19ED-6 Change in Energy due to Superheat

	Change in Energy (%)		
Superheat (°C)	Scenario I	Scenario II	Scenario M
0	0	0	0
5	2	1	1
10	3	3	3
25	8	7	7
50	15	14	14
100	31	27	29
125	39	34	36
150	~	41	~

Table 19ED-7 Plug Formation Times with Superheat

	Plug Formation Time (sec)		
Superheat (°C)	Scenario I	Scenario II	Scenario M
0	5.7	4.2	4.2
5	5.9	4.3	4.3
10	6.1	4.4	4.4
25	6.7	4.8	4.8
50	7.7	5.4	5.4
100	9.9	6.7	6.9
125	11.1	7.5	7.7
150	~	8.3	~

Table 19ED-8 Required Channel Lengths with Superheat

	Required Channel Length (m)		
Superheat (°C)	Scenario I	Scenario II	Scenario M
0	0.18	0.05	0.35
5	0.19	0.05	0.37
10	0.19	0.05	0.39
25	0.22	0.06	0.44
50	0.27	0.07	0.53
100	0.40	0.09	0.75
125	0.47	0.11	0.89
150	~	0.13	~

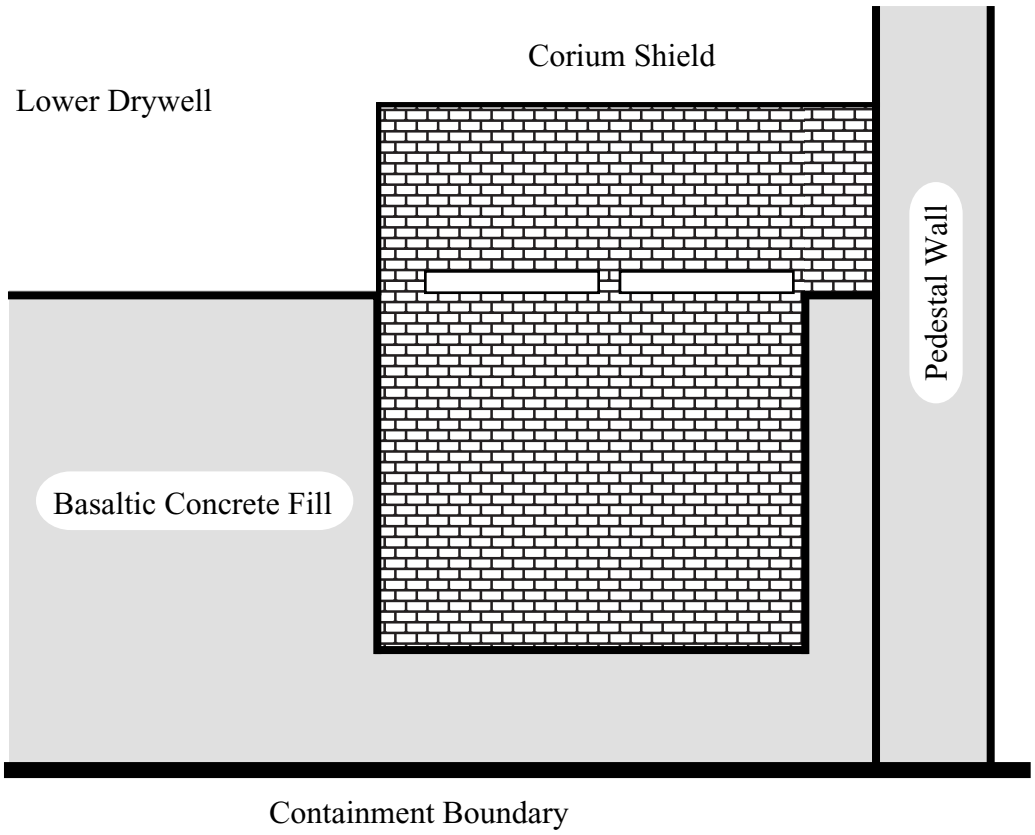

Figure 19ED-1 Conceptual Design of Lower Drywell Floor Drain Sump Shield

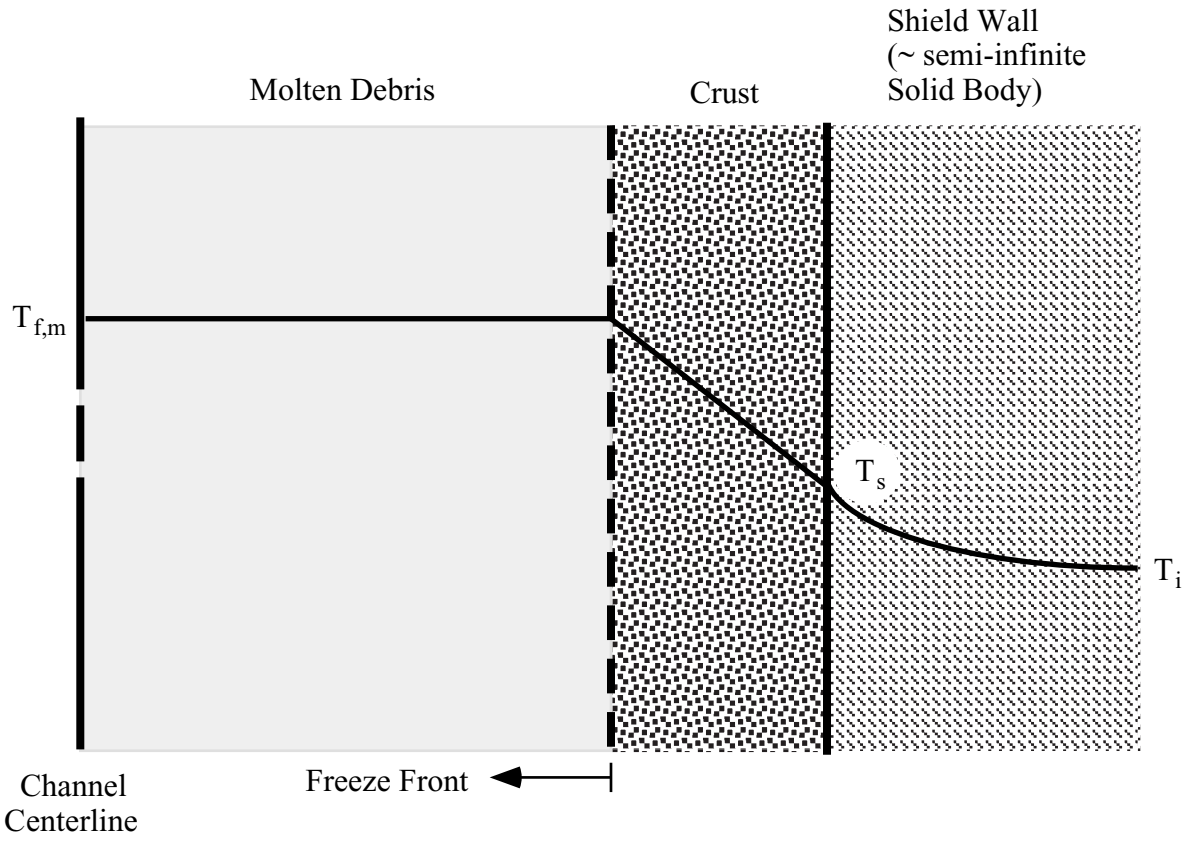

Figure 19ED-2 Temperature Profile in Channel Region

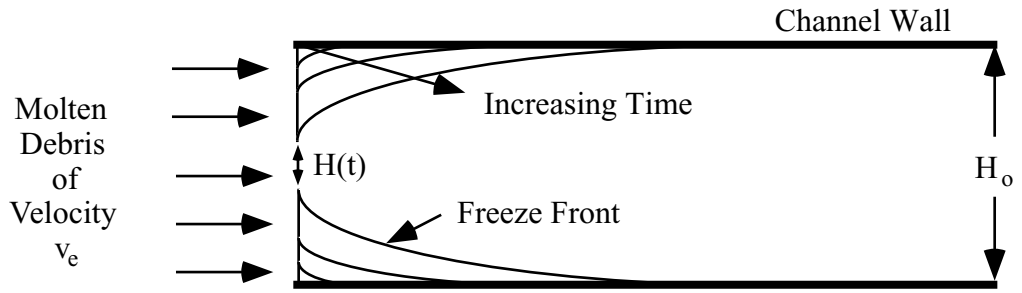

Figure 19ED-3 Channel Flow Height Reduction During Freeze Process